Simulations of radiative transfer in the SAPHIR and AMSU channels in the perspective of water vapor profiles retrievals

Sarah Franquet, Noelle Scott, Alain Chedin, Raymond Armante,
ARA/LMD Ecole Polytechnique, Palaiseau, France
Laurence Eymard, CETP, Velizy, France

Abstract

An approach based on Neural Networks is applied to retrieve atmospheric water vapor profiles and the total precipitable water from the Advanced TIROS-N Operational Vertical Sounder (ATOVS) and the Sondeur Atmospherique du Profil d'Humidité Intertropicale par Radiometrie (SAPHIR) channels. The validation of the forward radiative transfer model used to construct the training data set is based on real observations from NOAA-15 and NOAA-16. Humidity retrievals from the radiances observed by the 20 channels of the AMSU instrument are made on a global scale over sea and near nadir for the first applications. Comparison with other algorithms shows the good quality of this approach although other tests should be done for a more complete conclusion.

1 Introduction

The Advanced Tiros-N Operational Vertical Sounder (ATOVS) is composed of the Advanced Microwave Sounding Unit (AMSU) and the High-resolution Infrared Radiation Sounder (HIRS/3) and flies on board the National Oceanic and Atmospheric Administration (NOAA) polar-orbiting satellites. NOAA-15 and NOAA-16 were launched on May 1998 and September 2000 respectively.
The AMSU (AMSU-A and AMSU-B radiometers) has 20 channels in the microwaves. The AMSU-A is a cross-track, line-scanned instrument (15 discrete frequency channels) aimed at retrieving temperature profiles. It has an instantaneous field-of-view of 3.3 degrees at the half-power points providing a nominal spatial resolution at nadir of 50 km (30 contiguous scene resolution cells). The AMSU-B is a cross-track, continuous line scanning, total power radiometer with an instantaneous field-of-view of 1.1 degrees (at the half-power points). Spatial resolution at nadir is nominally 16 km (90 Earth fields-of-view per scan line). Its purpose is to obtain global data on humidity profiles. It works in conjunction with the AMSU-A instrument.
The Sondeur Atmospherique du Profil d'Humidité Intertropicale par Radiometrie (SAPHIR, in project for a tropical orbit) has six channels symetrically disposed around the water vapor absorption line at 183.31 Ghz as the channels 18, 19, and 20 of AMSU (the last three channels of AMSU-B). It is a transverse cross-track instrument with a spatial resolution at nadir of 10-12 km.
The approach used to retrieve atmospheric water vapor profiles from the SAPHIR and AMSU channels is then similar and accounts for the non linearity between water vapor content and the radiometer observations: it relies on neural netwoks.
We first present the method used. The next section is dedicated to the training phase with the description of the forward model and its validation based on real observations from NOAA-15 and collocated radiosondes on one side, from NOAA-16 and operational NOAA retrievals on the other side. We then apply the retrieval scheme to water vapor retrievals and compare our results to those from other algorithms.

2 The Neural Network approach to retrieve water wapor profiles

The use of Neural Networks (NN) in statistical estimation is often effective because they can simultaneously address nonlinear dependencies and complex statistical behavior. The strong nonlinear dependence of 183 GHz brightness temperatures on water vapor suggests that NN may be favorably used. NN have been successfully used for water vapor retrievals with TOVS instruments (Chaboureau, 1997) and ATOVS intruments (Cabrera-Mercater and Staelin, 1995). The system proposed here is the multi-layer perceptron (MLP). A schematic of the network is shown in Figure 1.

It is a non linear mapping model composed of parallel processors called 'neurons'

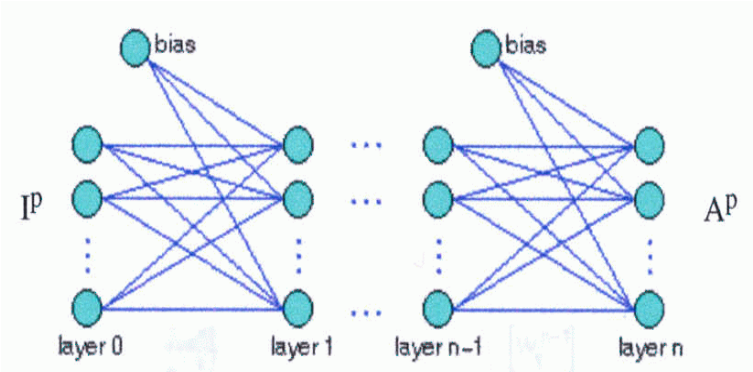

Figure 1: MLP architecture, Ip:input layer, Ap:output layer

organized in distinct layers : the first layer represents the input of the mapping. The intermediate layers are called the 'hidden layers'. These layers are connected via neural links : two neurons i and j between two consecutive layers have synaptic connections associated with a synaptic weight w_{ij}. One neuron i executes two simple operations. It makes a weighted sum of its inputs z_i, activity of the neuron :

$$a_j = \sum_{i \in Inputs(j)} w_{ij}.z_i$$

Then, it transfers this signal to its output through a so called 'transfer function', often a sigmoide function such as $\sigma(a) = tanh(a)$. The output z_j of neuron j in the hidden layer is then given by :

$$z_j = \sigma(a_j) = \sigma(\sum_{i \in Inputs(j)} w_{ij}.z_i)$$

Given a neural architecture (number of layers, neurons and connections), all the information of the network is contained in the set of synaptic weights $W = \{w_{ij}\}$. The learning algorithm is the optimization technique that estimates the optimal network parameters W by minimizing a loss function for a set of representative patterns for which inputs and ouputs are known (the learning set) to approach as close as possible the desired function by the neural mapping. Here the Error Back-Propagation algorithm (Rumelhart et al., 1986) is used to minimize this function. It is a gradient descent algorithm well adapted to the MLP hierarchical architecture because the computational cost is linearly related to the number of parameters. To avoid local minima during the minimization of the criterion, stochastic steepest

descent is used. The learning step is made for only one sample chosen iteratively and stochastically in the learning data set.
Here we are considering the retrieval of total precipitable water (TPW) and water

vapor profiles.
Two hidden layers are used in the network, each having 40 neurons. The hidden neurons are nonlinear with hyperbolic tangent activation functions and the output neurons are linear. The input to the network is a vector of the 20 channels of AMSU (the sounding channels of AMSU A provide temperature profile information necessary to interpret the humidity profile information contained in the water vapor channels). For each input vector the system produces estimates of TPW or water vapor profile at five layers (100-300, 300-525, 525-725, 725-850, 850-1013 mb). and the quality of the restitution is related to the quality of the modelisation. The next section describs the validation of the forward model.
The first on the synthetic 'TIGR 2000', then NOAA-NESDIS) and against

3 Construction of the training dataset

3.1 The training data set

The training set as defined above is presented to the network repeatedly until the retrieval error for these data converge to a minimum. The training set is constructed using the 2311 radiosondes from TIGR 2000 (Thermodynamic Initial Guess Retrieval, Chedin et al., 1985; Achard, 1991; Chevallier et al., 1998). The nominal number of pressure levels is fourty between the surface and 0.05 mb. The database is composed of the temperature (K), water vapor (g/g) and ozone (g/g, UGAMP Climatology, Li and Shine, 1995) profiles. The brightness temperatures are computed by the forward model at the frequencies of the AMSU (or SAPHIR) channels and the corresponding TPW or water vapor profile for each atmosphere in the training set were presented to the network during the training. To account for instrument noise, a pseudo-random number generator was used during training to introduce random variations in the simulated brightness temperatures.
The training phase of the method implied the use of a forward model and the quality of the restitution is linked to its quality.

3.2 Description of the forward model

The forward model is a line-by-line model using Liebe 1993 spectroscopic data (oxygen absorbtion lines, water vapor lines and continuum). In the current version, the Zeeman effects are not taken into account. We represent the emissivity over land at all frequencies by a constant value e.g. 0.95 but here we are considering situations over ocean. The emissivity is then computed from Stephen English's fast code which parameterizes an effective surface emissivity and reflectivity (FASTEM2 'simplified'), an approach based on that of Petty and Katsaros (1994). It computes the emissivity averaged over all facets representing the surface of the ocean and an effective path correction factor for the downwelling brightness temperature. The latter is different for each polarization.
FASTEM2 is devised to first calculate the specular emissivity using a physical model (geometric optics based on the Cox and Munk (1954) sea-slope variance model) and then add a roughness correction which is calculated by regression using predictors (including parameters which could influence the change in emissivity due to roughness (windspeed, view angle)). The specular component is calculated us-

ing Fresnel theory using a Debye model of the permittivity based on laboratory measurements. The recent dielectric model of Lamkaouchi et al (1997), based on laboratory measurements up to 100 GHz is used. A simple term has been added to account for enhancement of the emissivity by Bragg scattering following Choudhury et al. (1979) and the effect of foam has also been simply accounted for using the formula of Monahan and O'Muircheartaigh (1986).
The model is devised to provide an estimate of emissivity for any channel between 10 and 200 GHz for any view geometry up to 60 degrees and windspeeds from 0 to 20 ms-1. It has been validated against airborne radiometers flown on the UK Met. Office C-130 aircraft (Guillou et al. 1996).

3.3 Validation of the forward model on AMSU A and B channels

The model is tested on NOAA-15 and NOAA-16 data. Some results are presented in Figure 2.
For the NOAA-15, it is the ATOVS Sounding Product (May 99 - Oct 2000), global : Radiosonde Match Archive which contains radiosonde and retrieval data collocated in time and space. Only the AMSU A channels can be considered as no AMSU B brightness temperatures are available in this file. The number of clear situations is 88 668 matchups. There are few holes over the period; it is composed of 13 months with an average of 512 matchups each.
For a sea and day flag of the satellite, the number of matchups for the whole period reduces to 21 607. After 'quality control' on the radiosonde data (minimum pressure of the temperature profiles : 30. hPa, of the water vapor profiles : 350. hPa; minimum number of levels for the temperature : 20; minimum number of levels for the water vapor : 10) and with the equivalent sea flag of the radiosonde, the number of matchups becomes 6 672 over the period. The temperature and water vapor profiles of the radiosondings are interpolated and extrapolated on the basis of 47 levels from 0.03 mb to the surface pressure.
Figure 2(top) shows an example of results for the month of October 2000 (549 matchups). As expected, the bias and standard deviation for the sounding channels (channels 4 to 11 of AMSU A) are small, not being affected by the surface. The bias and standard deviation increase for the higher sounding channels (12 to 14). This is principally due to the fact that their weighting functions are sounding very high in the atmosphere when the extrapolated profiles stop at 0.03 mb. For the other channels of AMSU A (1 to 3 and 15), the bias and standard deviation are important because of the large impact of even small errors in the surface characteristics (emissivity, temperature).

For NOAA-16, we use the Retrieval Orbital Data File (RODF) of the NOAA-NESDIS for one day : November 29th, 2000 . Both the AMSU A and B channels can be now considered, Figure 2(bottom). We are still considering clear situations over sea but for view angles near nadir (2025 matchups). The temperature and water vapor profiles come from the NOAA retrievals. The fit of the calculated brightness temperatures with the observed brightness temperatures is significantly better and satisfactory for all the sounding channels of AMSU A (4 to 14). The bias and standard deviation are still important for the window channels of AMSU A (1 to 3, 15) but much less than for the previous set of data. It is worth pointing out that, because we are using retrievals, there is no time and space difference with the satellite. The results for the AMSU B channels seem reasonable. Situations with all view angles have also been tested. Three orbits were used (again from November 29th, 2000 giving 2640 matchups). The statistics for the sounding channels 4 to

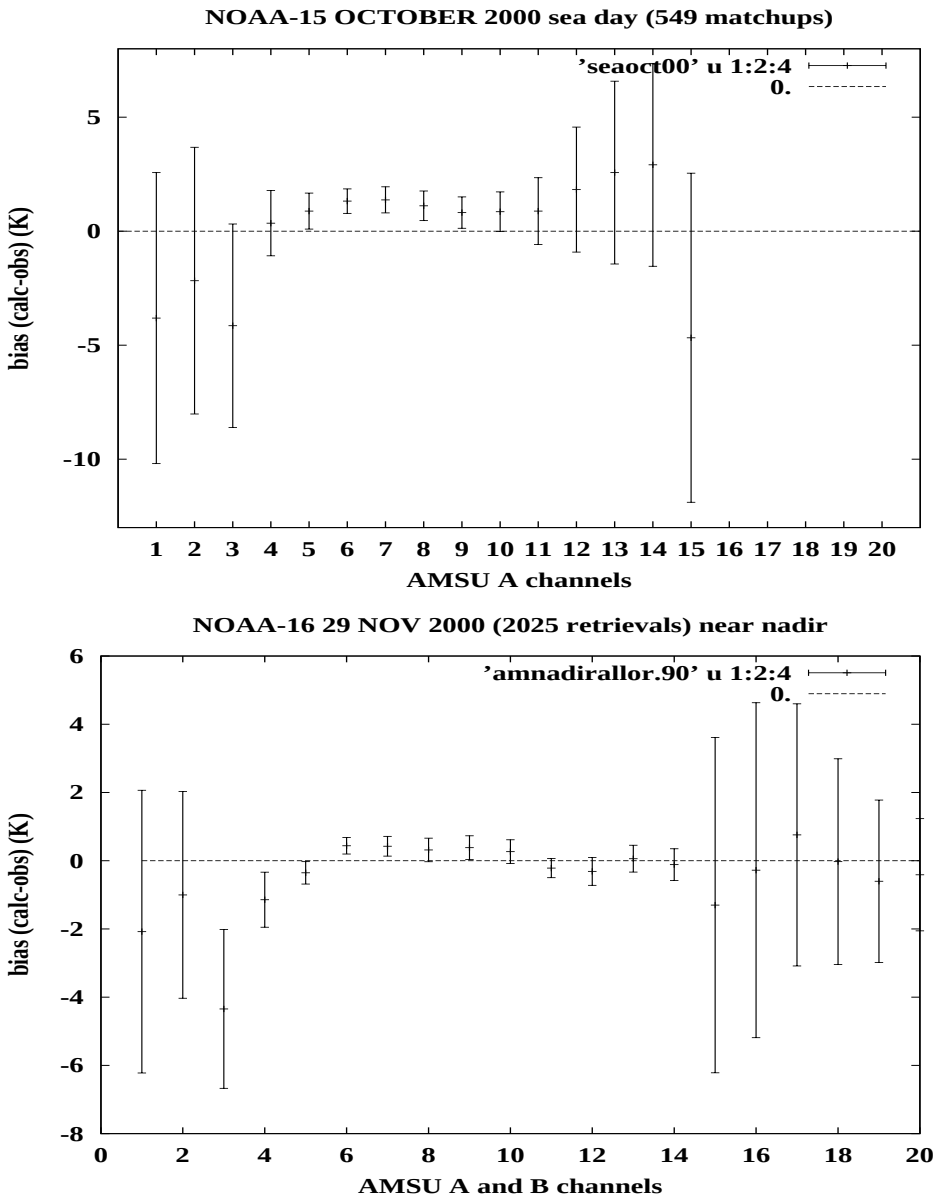

Figure 2: Biases of the forward model on AMSU A and B channels for NOAA-15 (top) and NOAA-16 (bottom) observations

14 of AMSU A are still stable and constant. The bias is low around zero and the standard deviation is of the same order. For the other channels (window channels) the bias and the standard deviation are significant. The sign of the bias has changed for almost all channels and its value is of the same order as the results at nadir.
Having validated the model over two different sets of data, we can be quite confident for the sounding channels and conscious of potential errors resulting from the use of the window channels.

4 Application of the MLP model to the retrieval of Total Precipitable Water and water vapor profiles

For the NN applications, three types of validation have been made. The first on the synthetic 'TIGR 2000', second and third with real observations against another algorithm for calculation of the TPW (N. Grody, NOAA-NESDIS) and against NOAA-NESDIS retrievals.

4.1 Total Precipitable Water

Table 1 gives the results obtained at the end of the training of the neural network. They are divided into the five atmospheric airmass classes of the TIGR database. As expected, biases and standard deviations are very low.

	nb atm	TPW (cm)	RMS (cm)	BIAS (cm)
Tropical	872	3.82	4.82E-2	1.35E-3
Mid-lat 1	388	1.22	3.28E-2	2.67E-3
Mid-lat 2	354	0.75	3.13E-2	4.81E-3
Polar 1	104	0.23	3.70E-2	4.56E-3
Polar 2	593	0.31	3.50E-2	5.89E-3

Table 1: TPW restitution on TIGR 2000 in the learning phase

The NN has been educated with all the AMSU channels. To test it on real observations we have considered the RODF (November 29th 2000) of NOAA-16, which provides brightness temperatures observed and the corresponding TPW retrieved by the NOAA. Because the first education of the NN is made with nadir view angle, we are only considering near nadir observations (maximum view angle of 8.1 degrees from nadir).
The Grody's algorithm (Grody et al., 1999) for the TPW is part of the Microwave Surface and Precipitation Products System (MSPPS), Product Services Branch) of the NOAA-NESDIS. As described in Grody's paper, the precipitable water is obtained by regression with a set of coefficients (all of them display view angle dependence). An exact radiative transfer equation is used to determine the coefficients by simulating the AMSU measurements for clear and cloudy atmospheres, with sea surface winds varying between 0 and 15 m/s. The coefficients are determined by a least-squares fit of the simulated brightness temperatures to precipitable water. The optimal two-window channels used to retrieve precipitable water and cloud liquid water with equal accuracy has been found to be 23.8 GHz and 31.4 GHz e.g.

AMSU A 1 and 2 channels.
Figure 3 presents the comparisons for near nadir view angles because of the preliminary learning of the NN (present limit of the method, to soon being extended to all view angles). The number of retrievals is 2014 for the day November 29th, 2000. It drops to 1191 when considering the Grody's algorithm that identifies and removes sea ice contaminated scenes.
The first plot is the fit between the NN and the Grody's algorithm results. It presents the best agreement among the comparisons. We have already noticed between the value of TPW from the TIGR 2000 database and the TPW calculated with Grody's algorithm on the corresponding simulated brightness temperature a slight deviation for dry atmospheres. It seems the forward model has a tendency to find more humidity in the dryier classes than Grody's calculation. This point is confirmed by the second plot which presents the same deviation but with the NOAA retrievals for atmosphere with TPW below 1.5 cm. About the third plot, we can notice that the rms is significantly more important between Grody's TPW and NOAA retrievals than between Grody's TPW and the NN. Between NOAA retrievals and the NN both bias and rms are more important but the number of point is more important, there's been no preliminary test.
The NN first results for the TPW are encouraging and we are now presenting the primarly results for the water vapor profiles.

4.2 Water Vapor profiles

Results of the neural network training on "TIGR 2000" are presented for only two classes (Tropical (872 atm) and Polar 2 (593 atm) in Table 2 and 3 respectively).

Very good statistics are thus obtained on individual classes, although the network

pressure (mb)	$h2o\ TIGR2000$ (cm)	$h2o\ NN$ (cm)	RMS (cm)	BIAS (cm)
100-300	3.006E-02	2.980E-02	9.359E-03	-2.63521E-04
300-525	0.286	0.283	4.718E-02	-2.385E-03
525-725	0.801	0.805	8.910E-02	3.743E-03
725-850	0.917	0.922	0.108	4.759E-03
850-1013	1.777	1.771	9.296E-02	-5.279E-03

Table 2: Tropical classe of TIGR 2000

pressure (mb)	$h2o\ TIGR2000$ (cm)	$h2o\ NN$ (cm)	RMS (cm)	BIAS (cm)
100-300	1.852E-03	1.656E-03	1.793E-03	-1.965E-04
300-525	1.865E-02	1.869E-02	7.871E-03	3.981E-05
525-725	7.138E-02	7.270E-02	2.789E-02	1.312E-03
725-850	8.263E-02	8.519E-02	1.920E-02	2.564E-03
850-1013	0.135	0.135	3.160E-02	-4.923E-04

Table 3: Polar 2 classe of TIGR 2000

was trained on the whole TIGR dataset.

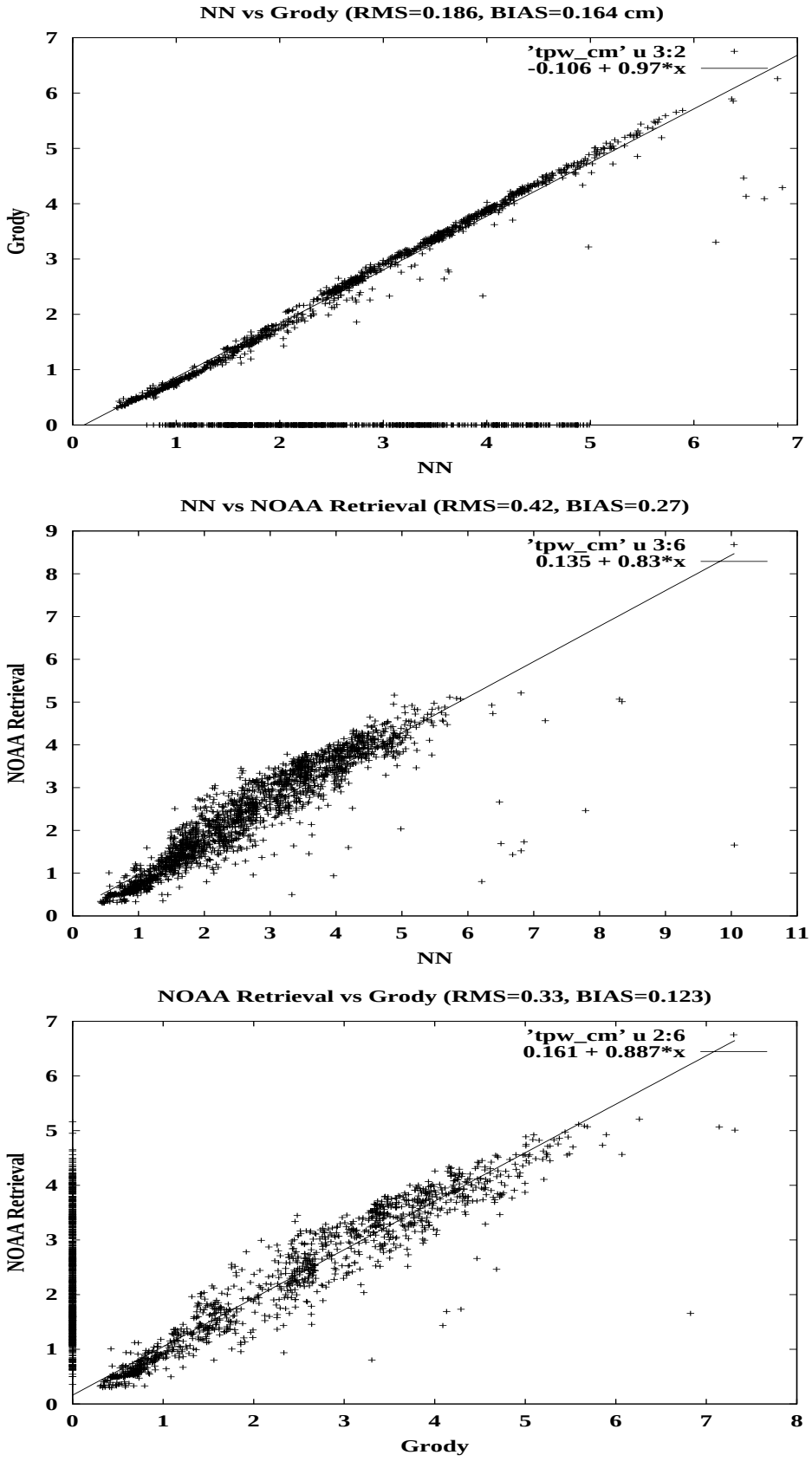

Figure 3: Comparisons of TPW retrievals (cm): (top) Grody against NN, (middle) NOAA retrievals against NN, (bottom) NOAA retrievals against Grody. The TPW is set to 0 whe n Grody's algorithm flags sea ice

pressure (mb)	$\bar{h2o\ set1}$ (cm)	$\bar{h2o\ set2}$ (cm)	$\bar{h2o\ set3}$ (cm)	$\bar{h2o\ total}$ (cm)
100-300	0.006	0.007	0.010	0.007
300-525	0.042	0.094	0.191	0.088
525-725	0.163	0.436	0.762	0.378
725-850	0.265	0.730	1.075	0.600
850-1013	0.739	1.791	2.344	1.465
$\bar{TPW}$ (cm)	1.212	3.055	4.377	2.535

Table 4: Mean values for the water vapor profiles (retrievals of the NOAA) for the three sets and the whole set of situations (2025)

To test the neural network on real observations (using all the AMSU channels), we use the NOAA-16 RODF. So we may compare the water vapor profiles resulting from the NN to the NOAA retrievals. It is a set of 2025 atmospheres. In order to keep the qualitative aspect of the result, we have divided the data into three sets, the division being made with respect to the value of TPW retrieved by NOAA. The first set has values of TPW between 0. to 2. cm (783 atmospheres), the second between 2. to 4. cm (947 atmospheres) and the last one between 4. to 7. cm (295 atmospheres). Below is the list of the mean values of the water vapor profiles for the different sets and for the whole set (Table 4). For each set, the rms and bias for the difference between the NN algorithm and the NOAA retrievals are shown on Figure 4.
The rms is quite stable along the pressure profile for all airmass sets of data: it slightly increases with the mean TPW of the sets. It is also more important near the surface for the same reason (the water vapor is more important there). On the contrary, the bias presents differences between the layers which grow with the different sets. For example, the bias of the near surface layer goes from 0.1 cm in the first set to about -0.1 in the second and then -0.3 in the third. The bias is more important for values of TPW larger than 4 cm. As we have no other way of comparison for the water vapor profiles, we have deduced the TPW from the retrieved water vapor profiles and from the NN profiles and we have compared them again with the Grody's algorithm results (Figure 5). In this set of data, the application of the sea ice test in the Grody's algorithm drops the number of atmospheres from 2025 down to 1191.
The dashed line is the previous linear regression fit (Figure 3) and the solid line is the current fit. We find the same kind of results than previously obtained, however slighlty better. Again, the dispersion with the NOAA retrievals is of the same order of magnitude and the fit between the Grody's algorithm application and the NN results is good.

5 From AMSU to SAPHIR

Preliminary tests have been made with SAPHIR and with AMSU-B channels and presented in previous SAPHIR (/Megha-Tropiques) conferences. In the nominal version of SAPHIR, it was planned to have 6 or 7 channels with the aim of sounding the largest possible layer of the atmosphere between surface and low pressure with the best vertical resolution. By a lot of numerical experiments with the above mentioned forward model, we have been working to define while avoiding forbidden channels the best combination of number and location of the channels in order to fulfill this requirement. The current version of SAPHIR is six channels with two

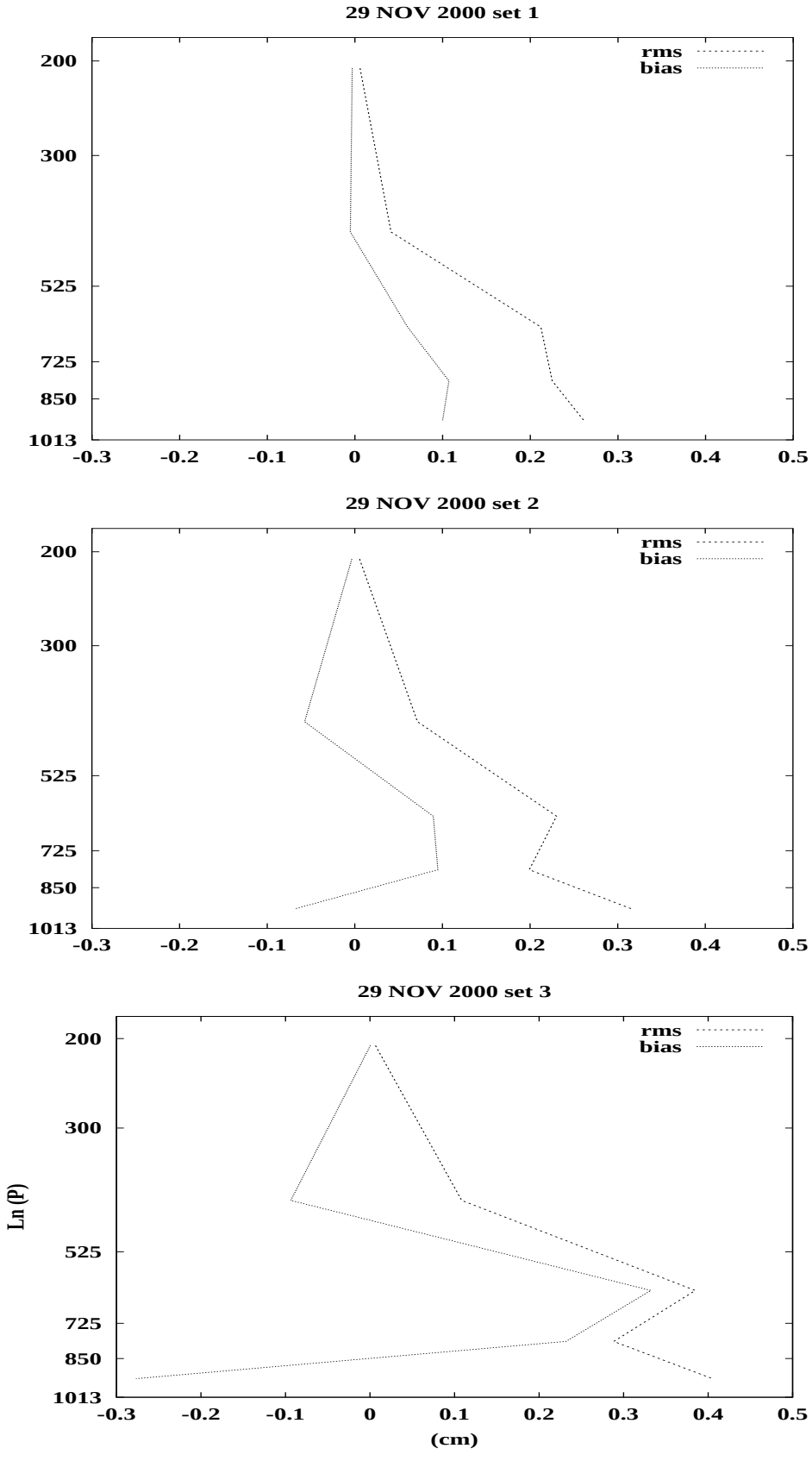

Figure 4: rms and bias for water vapor profiles (NN-NOAA retrievals)

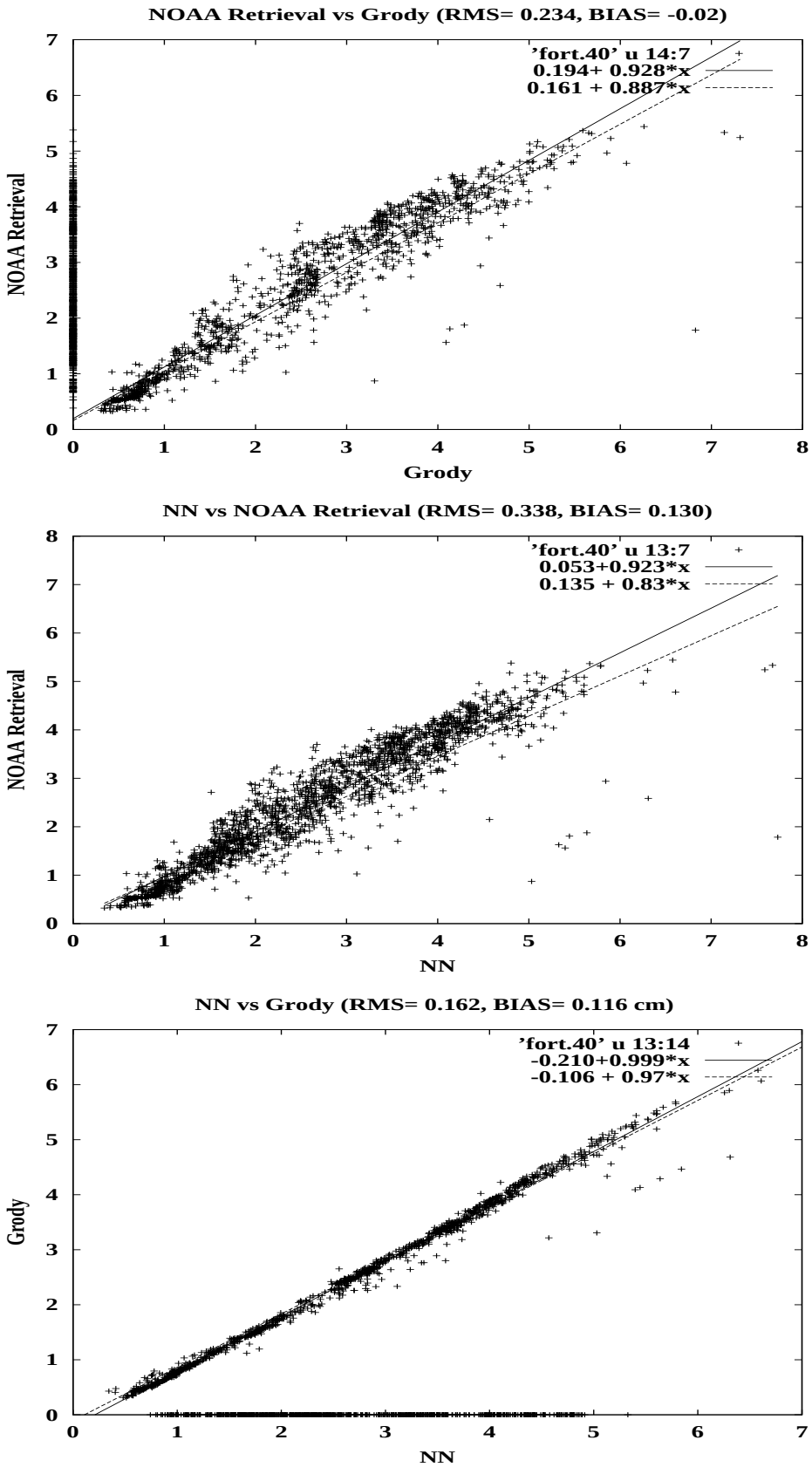

Figure 5: Comparisons of TPW retrievals (cm): (top) Grody against NN, (middle) NOAA retrievals against NN, (bottom) NOAA retrievals against Grody. The TPW is set to 0 when Grody's algorithm flags sea ice

arches symetrically disposed around 183.31 GHz (183.51, 184.51, 185.91, 187.31, 189.71, 192.41 GHz). The last comparisons with AMSU-B were made with the following status for the NN's:
For SAPHIR : brightness temperatures simulated for the channels (6), temperature profile (6 layers), surface temperature and TPW for the input layer; two hidden layers (15,15 neurons); humidity profile (6 layers) for the output layer. For AMSU-B : brightness temperatures simulated for the channels (5), temperature profile (5 layers), surface temperature for the input layer; one hidden layer (10 neurons, sufficient to obtain a good convergence of the mean water vapor rms); humidity profile (5 layers) for the output layer.
Results from SAPHIR, although quite identical to AMSU-B display significant improvements in layers between 850 and 450 mb. The rms for SAPHIR was quite dependent of the layering and it was improved by the introduction of the TPW in the input layer of the network.

6 Conclusion

We have developed a Neural Network (NN) approach for retrieving water vapor profiles and TPW. The training data set is based on the TIGR-2000 climatological data set for its atmospheric component and on a microwave forward model, validated against real observations from NOAA-15 and NOAA-16, for its brightness temperature component. The forward model gives good agreement for the sounding channels. Channels sensitive to the surface, particularly over sea, are still difficult to simulate accurately due to remaining problems with the modeling of the surface emissivity. Those channels are however used in the retrieval process due to the importance of the information content they carry. Comparisons with NOAA retrievals (TPW and profiles) and with Grody's algorithm (TPW) give confidence in our NN restitutions. Presently limited to near nadir view angles, the method is easily (and will be) extended to all view angles.
Work is continuing with the study of AMSU (or SAPHIR) in either a stand alone mode or coupled with the HIRS (ATOVS) instrument as well as with the Improved Atmospheric Sounder Interferometer (IASI) or the Atmospheric Infrared Radiation Sounder (AIRS) instruments. These studies should help constraining the final choices for the SAPHIR channels-characteristics.

Acknowledgments. Thanks are due to Ellen Brown and Antony Reale for useful discussions on the content of AMSU/NOAA-15 and NOAA-16 datafiles. Warmful thanks also to Norman Grody for his unrestricted help and patience when answering questions on his scientific approach and algorithms. Work concerning SAPHIR has been performed with the SAPHIR scientific team, we want to thank Maurice Gheudin, Gérard Beaudin.

References

Achard, V., 1991. Trois problemes clés de l'analyse 3D de la structure thermodynamique de l'atmosphere par satellite. PhD thesis, Université Paris 7, 168 pp.

C. Cabrera-Mercater and D.H. Staelin, 1995: Passive microwave relative humidity retrievals using feedforward Neural Networks, IEEE Trans. On Geoscience and Remote Sensing , 33, 1324-1328.

Chaboureau, J.-P., A. Chedin, and N. A. Scott, 1998: Remote Sensing of the vertical distribution of atmospheric water vapor from the TOVS observations. Method and validation. J. Geophys. Res., 103, 8743-8752.

Chedin, A., N.A. Scott, C; Wahiche, and P. Moulinier, 1985. The improved ini-

tialization inversion method : a high resolution physical method for temperature retrievals from satellites of the TIROS-N series. J. Climate Appl. Meteor., 24, 128-143.

Chevalier, F., F. Cheruy, N.A. Scott, and A. Chedin, 1998. A neural network approach for a fast and accurate computation of a longwave radiative budget. J. Appl. Meteor. ,37, 1385-1397.

Choudhury, B.J., T.J. Schmugge, A. Chang and R.W. Newton, 1979: Effect of surface roughness on microwave emission from soils. J. Geophys. Res. 84, 5699-5706.

Cox, C., and W. Munk: Statistics of the sea surface derived from sun glitter, J. Marine Res., 13, 198-226, 1954.

Ellison, W., A. Balana, G. Delbos, K. Lamkaouchi, L. Eymard, C. Guillou et C. Prigent, New permittivity measurements of sea water, Radio Science, 33, 639-648, 1998.

English, S.J., and T.J. Hewison, 1998: A fast generic millimeter-wave emissivity model, Proceedings of SPIE, 3503, 288-300.

Grody N., Weng F. and Ferraro R., 1999 : Application of AMSU for obtaining water vapor, cloud liquid water, precipitation, snow cover and sea ice concentration. ITSC-10, Boulder, Jan 27-Feb 2.

Guillou C., English S.J., Prigent C., Jones D.C., Passive microwave airborne measurements of the sea surface response at 89 and 157 GHz, J. Geophys. Res. 101, 3775-3788, 1996.

Li, D., and K.P. Shine, 1995. A 4-dimensional ozone climatology for UGAMP models. UGAMP Internal Report No. 35, April 1995.

Liebe, H.J., P.W. Rosenkranz and G.A. Hufford, 1992: Atmospheric 60 GHz oxygen spectrum: new laboratory measurements and line parameters, J. Quant. Spectros. Radiative Transfer, 48, 629-643.

Monahan, E. C., and I. G. O'Muircheartaigh, Whitecaps and the passive remote sensing of the ocean surface, Review article, Int. Remote Sens., 7, 627-642, 1986.

Petty, G.W. and K.B. Katsaros, 1994: The response of the SSM/I to the marine environnement. Part II: A parametrization of the effect of the sea surface slope distribution on emission and reflection, J. Atmospheric and Oceanic Technology, 11, 617-628.

Rumelhart, D.E., G.E. Hinton, and R.J. Williams, 1986. Learning internal representations by error propagation. Parallel distributed processing : explorations in the macrostructure of cognition l., D.E. Rumelhart and McClelland, Eds, MIT Press, 318-362.

Zhao J., Grody N., Ferraro R., Zou C. and Weng F., 2000 : The new NOAA AMSU hydrological product suite : the validation of AMSU TPW and CLW. American Meteorological Society 196-199.